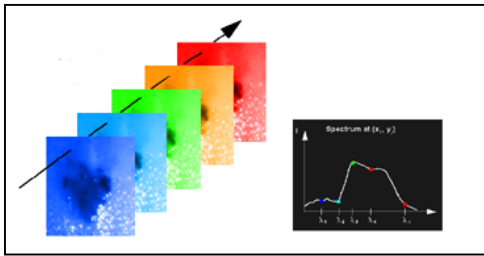


# Spectral imaging and microscopy

Richard M. Levenson and Clifford C. Hoyt

## Spectral Imaging

In biomedicine, color is frequently used to increase information content. Traditionally, in the guise of histological stains, color signals the biochemical makeup of different regions of tissue, most typically, nuclei vs. cytoplasm. When coupled to more precisely targeted indicators, such as



**Figure 1.** A spectral cube consists of a number of grayscale images showing intensity at every pixel as a function of wavelength. An optical spectrum is thus associated with each pixel.

antibodies and nucleic acid probes, colors can allow the detection of multiple, highly specific analytes. However, our native ability to perceive and evaluate color information is somewhat constrained because, by definition, we are limited to the visible range in terms of wavelengths, and because we (and our conventional RGB cameras) are suboptimal in terms of spectral resolution: all spectral information, no matter how complex, is binned into about 3 broad spectral ranges roughly corresponding to red, green and blue. Spectral imaging is a relatively novel technique which uses precise measurements of optical spectra at every pixel of an image in order to overcome these deficiencies and thereby to appreciate differences in color that might otherwise

be inapparent. Sophisticated algorithms can be used for the extraction of maximum information from the analyzed scenes. We find that when general histology stains are used, spectral analysis can uncover unseen specificities in staining behavior. And when specific probes are applied to tissue, spectral imaging can help disentangle multiple colors, even when they overlap either spectrally, spatially, or both.

## Spectral Imaging Methods

A spectral dataset generally consists of a number of images representing brightness at each pixel as a function of wavelength. As shown in Figure 1, the data can be represented as a cube with dimensions  $x, y$  and wavelength with an optical spectrum associated with every pixel. There are a number of ways to acquire spectral data sets that are all capable of providing useful information. Naturally, each method has its own set of advantages and disadvantages. In addition to relatively inflexible multi-position filter wheels, current methods include tunable illumination, Fourier-transform imaging spectroscopy and various forms of tunable bandpass filtering.

Most spectral imaging systems filter the imaged light (either transmitted or emitted), but some approaches can vary the illumination source. Thus, with a tunable light source, the illuminating light is scanned continuously or discontinuously through a number of wavelengths. A grayscale image is taken at each desired wavelength and the resulting image stack constitutes a spectral cube. This method benefits from simplicity, (relatively) low cost, and from the fact that no additional optical or mechanical elements are interposed in the imaging light path, resulting in minimal image degradation. The light sources can be tuned either using diffraction gratings, used in most monochromators, or electronically tunable filters, such as acousto-optic tunable filters (AOTFs) or liquid crystal tunable filters (LCTFs). This technique is good for brightfield only; it does not provide spectral discrimination for fluorescence-based applications.

In Fourier-transform imaging spectroscopy, commercialized by Applied Spectral Imaging (ASI), light from the object passes through the microscope objective to enter a Sagnac interferometer which splits it into two beams. These beams are sent in opposite directions around a common light path and are allowed to interfere with one another after a small and variable optical path difference (OPD) has been introduced. The resulting interference pattern is then focused onto a cooled CCD detector. An interferogram at each pixel is generated by optically changing the OPD and recording the digitized signals of successive frames. The computer then calculates the spectra using a fast Fourier transform (FFT).<sup>1</sup> Maximum image size is limited by computational considerations to about 500 x 500 pixels in the instruments currently mounted onto light microscopes. The cost of the commercially available units (\$75K and up, exclusive of microscope) is also a consideration.

Tunable filters come in three flavors: continuously variable circular filters (CVFs) which are rotated to select the spectral bandpass; and acousto-optical and liquid crystal devices. CVFs pose problems in that any imaged field will have a spectral gradient superimposed on it. With an acousto-optical tunable filter (AOTF), filtered light of narrow spectral bandwidth is angularly deflected away from the incident beam at the output of the crystal. The central wavelength of this filtered beam is determined by the acoustic frequency of the AOTF; this wavelength can be changed within approximately 25 ns to any other wavelength. However, the technology suffers from some drawbacks that have limited its use in microscopy, principally those of poor light budget, and image blur and shift. Some technical solutions have been proposed,<sup>2</sup> but these do not address all the problems.

Liquid crystal tunable filters (LCTF), like AOTFs, permit the acquisition of a series of images over a range of wavelengths using no moving parts. LCTFs use electrically controlled liquid crystal elements that transmit a certain wavelength band while being opaque to others. The rejection of the unselected wavelengths, without further manipulation, is about 10<sup>4</sup>:1.<sup>3</sup> The bandpass can be as narrow as 1 nm and the spectral range of a typical device operating in the visible range is 420 to 720 nm. Similar LCTF configurations can provide tunable filtering into the near IR up to 1.7 microns. Continuously tunable LCTFs can be switched from wavelength to wavelength in about 50 milliseconds (faster units which toggle between defined states within 1 millisecond), and are optically well behaved in that they do not induce image distortion or image shift. Image size is limited only by the resolution of the digital camera used. CRI, Inc. has recently introduced a new version of this technology, the FluoroSpec™ tunable filter, which uses polarizing beam splitters to harvest both polarization states. In combination with other technical refinements, this has increased the signal at the CCD by about 4-fold over CRI's previous tunable filters, making it suitable for use in fluorescence applications as well as for brightfield spectral imaging.

### *Spectral Imaging Analysis Algorithms for Spectrally Complex Scenes*

The reliable detection of malignant cells in stained tissue samples is still one of the most arduous and time-consuming tasks in pathology and is a typical example of a *pattern recognition* problem. In its most general case, the task of pattern recognition in images consists of three independent steps: 1) the objects contained in the image scene are separated from the background (image segmentation); 2) the characteristics of each object are quantified (feature extraction); and 3) each object is assigned to a generic target class (classification).<sup>4</sup> In many image analysis applications, the image segmentation step is bypassed by defining each pixel as an individual object. A large array of classification algorithms is available to automate this task.<sup>5</sup>

There are several approaches to classifying pixels in a spectral image. The simplest scheme uses a minimum squared error method to compare each pixel in the image with a set of reference spectra

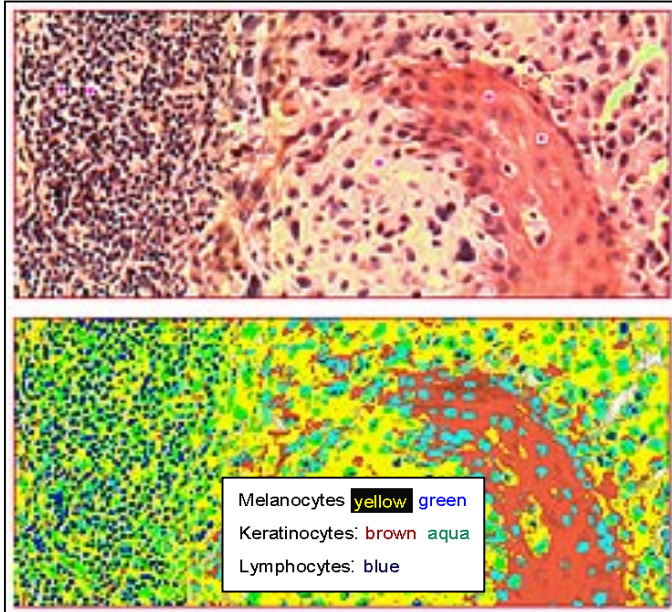


**Figure 2.** Spectral histochemistry . A spectral dataset of a formalin-fixed, paraffin-embedded, H&E-stained atypical nevus was acquired. **Top panel:** RGB-display of a spectral cube showing atypical melanocytes engulfing a portion of normal epidermis. An intense lymphocytic infiltrate is visible to the left. **Bottom panel:** Different cellular features can be classified using spectral signatures. The result is similar to that obtained with special immunostains.

using a least-squares criterion. Pixels are classified according to which pure spectrum they are most similar to and can be pseudo-colored to indicate the results of classification.<sup>6</sup> There are more advanced distance measures, such as Mahalanobis,<sup>7</sup> which can take into account variance among spectral classes. Determining which spectra to use for the classification procedure is not always straightforward. In simple cases, the reference spectra can be selected from obvious structures in the image (foci of cancer vs. normal cells, for example) or from established spectral libraries. Alternatively, informative spectra can be extracted using statistical analysis methods, such as principal component analysis (PCA) or clustering methods.<sup>8</sup> Instead of using a classified pseudo-color display, spectral similarity can also be illustrated by mapping the degree of similarity using gray-scale intensity. This operation can reveal otherwise inapparent morphological details.<sup>1</sup>

Frequently, classification or clustering is not performed directly on the raw input data, but on some linear transformation of the latter instead, typically the output of principal component analysis (PCA). This procedure has two advantages: first, the transformation of the original image data results in data that is typically better suited for subsequent classification. Second, a compression of the input data is achieved, which, given the high data volumes of modern image acquisition systems, is often a very desirable option.<sup>9</sup> PCA is exclusively based on the information contained in the covariance matrix of the input data. The covariance is a so-called second-order statistic, which takes only relationships between pairs of pixels in the input data into account. Higher order structures that depend on more than two pixels, such as edges, can therefore not be detected by PCA.<sup>10,11</sup> Given these shortcomings, image transformations that explicitly incorporate higher-order statistics to obtain a meaningful representation of the image data may prove to be a promising area of algorithm research.

### *Pixel Unmixing*

When pixels can be or are composed of more than one spectral class, as is often encountered when multiplexed protein or nucleic acid probes are used, then the pixels, rather than being classified, have to be unmixed. A linear combinations algorithm can be used to unmix the signals arising from the pure spectral components. The linear combinations algorithm assumes

each pixel is made up of a combination of pure spectra. Given an appropriate set of standards, the algorithm can quantitate the absolute amount of each label present.<sup>12</sup> The linear combinations

algorithm can only be applied in situations where the pure spectra combine linearly. This property holds for fluorescence images, but transmission and reflectance images must be converted to optical density before applying the linear combinations algorithm.

### *Applications of spectral imaging in biomedicine*

The mainstay of the field of pathology remains the microscopic examination of fixed and stained slices of tissue. Routine histopathology relies on staining with hematoxylin and eosin (H&E); although these dyes have certain affinities for cellular constituents, they are non-specific. Cytopathology specimens, including cervicovaginal Pap smears, are usually stained with other dyes, including the Romanowsky-Giemsa formulation (azure B and eosin Y) and the Papanicolaou stain (hematoxylin, orange G, eosin Y and light green), which generally create a wider variety of colors than are generated by classical H&E. Changes in cellular constituents that accompany inflammation and neoplasia and other physiological and pathological processes affect the distribution, intensity and color of the stains (for example, see Frable<sup>13</sup>).

Diagnostically important spectral features can be subtle and not easily assessed by the naked eye. However, using spectral imaging techniques, we have been able to distinguish cellular types from one another, including neoplastic vs. normal cells of the same cellular lineage.

Figure 2 illustrates the potential utility of spectral classification, using a minimum-square-error classification

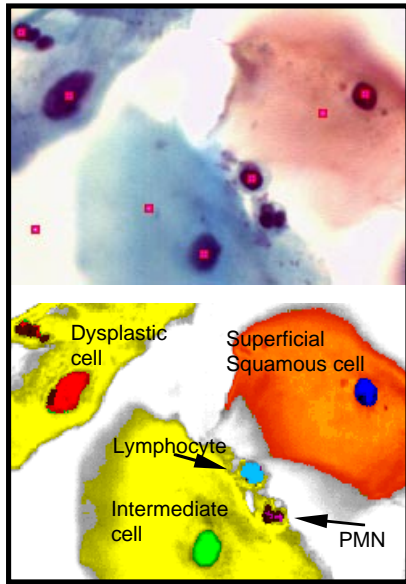


**Figure 3. Top panel:** An RGB-display of a spectral cube taken of Papanicolaou-stained cervicovaginal smear (Pap-smear). **Bottom panel:** Using reference spectra, the image was classified and pseudo-colored on a pixel-by-pixel basis. The cytoplasmic regions are clearly distinguishable from the nuclear regions, and the individual cell nuclei themselves form distinct spectral classes.

algorithm, to analyze conventionally stained pathology specimens. The tissue is skin obtained from a biopsy of an atypical melanocytic nevus (a possible precursor lesion for melanoma), routinely processed and stained with hematoxylin and eosin. The upper large panel consists of an RGB-representation of the spectral cube obtained by scanning the specimen over the wavelength range 400-700 nm with a Sagnac imaging interferometer using a 10X microscope objective. The lower panel shows the result of spectral classification using a least-squares metric. Spectral signatures of melanocyte nuclei and cytoplasm, keratinocyte nuclei and cytoplasm and lymphocyte nuclei are sufficiently distinct that the various compartments can be identified, spatially located and enumerated, without the use of special stains or intensive, hands-on operator involvement. This may be of great use in standardizing the evaluation of melanocytic penetration into skin compartments (vertical penetration into the dermis), since sometimes it is difficult to assess the extent of involvement (individual melanocytes may be hard to discern by eye whereas they can be detected spectrally).

Spectral analysis of a cervico-vaginal Pap smear is shown in Figure 3. The top panel contains an synthetic RGB image (derived from the full spectral dataset) of Papanicolaou-stained cervical smear containing squamous epithelial cells (a normal superficial cell, several normal intermediate cells and a mildly dysplastic cell). Also present in the image are a lymphocyte and 2 polymorphonuclear neutrophils (PMNs) normal inflammatory cells. Regarding color alone, the

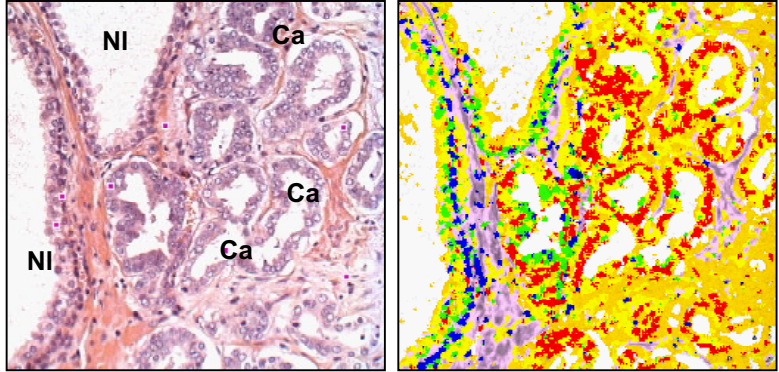


**Figure 4.** Spectral segmentation of a formalin-fixed, paraffin-embedded, H&E-stained prostate section (20 $\times$ ). **Left panel:** An RGB-rendering of the spectral datacube (NI: normal; Ca: cancer). **Right panel:** spectral segmentation is shown. *Green:* normal epithelial nuclei; *blue:* basal cell nuclei; *red:* cancer cell nuclei; *pink:* stroma; *yellow* and *tan:* epithelial cytoplasm.

nuclei of these cells, with the exception of the superficial cell (colored red-orange by orange keratin staining), are largely indistinguishable. Small squares in several nuclei indicate regions used to determine reference spectra to be used in spectral classification. The lower panel shows the result of image classification on a pixel-by-pixel basis using reference spectra and pseudo-colors. The cytoplasmic regions are clearly distinguishable from the nuclear regions, and the individual cell nuclei

themselves form distinct spectral classes.

Prostate cancer cells can be spectrally detected in images of prostate biopsy tissue stained with hematoxylin and eosin. This capability could be useful, for example, in automated screening of

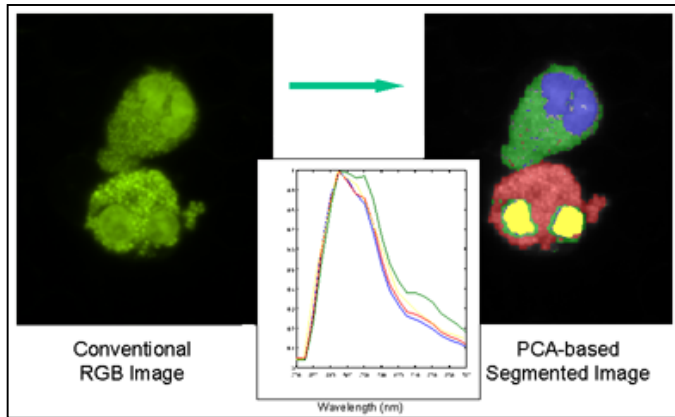


**Figure 5.** Spectral segmentation using a single dye. White blood cells differing in maturation state were stained using only one proprietary fluorescent dye and spectrally imaged using a CRI VariSpec<sup>™</sup> tunable filter. By eye, only slight differences in intensity (not hue) were visible. However, using PCA, 4 spectrally distinct regions could be discerned, corresponding to the nuclei and cytoplasm of each cell.

prostate chips removed for benign prostatic hyperplasia (BPH). Large volumes of tissue have to be examined in a search for potentially tiny foci of clinically unsuspected cancer. Figure 4 demonstrates that it is possible to spectrally separate malignant and normal epithelial cells, and to detect basal cells as well (these are a second cell layer found in normal prostate glands but absent in cancer). The segmentation is not perfect. Some of the imperfections (such as isolated misclassified pixels) can be suppressed using image processing techniques. However, the limitations in the present case include the fact that only a minimum square error algorithm was used more work is needed to explore capabilities of alternative analytical tools.

Remarkably, spectral information can also be extracted even if only a single dye is used, because dye behavior can be spectrally, if subtly, complex. In Figure 5, obtained with a CRI VariSpec<sup>™</sup> liquid crystal tunable filter, a single fluorescent dye was used to stain two similar white blood cells in different stages of maturation. The spectral dataset was used to separately segment the nuclei and the cytoplasms of both cells even though the image, as perceived by the human eye or conventional RGB camera, revealed nothing except slight changes in intensity (hue appeared constant). The segmentation was accomplished using PCA.

### *Multicolor Immunohistochemistry*

Immunohistochemistry involves the detection of antigens using antibodies coupled to some kind of chromogenic readout system. In the past two decades the technique has become central to the practice of oncologic pathology since it can distinguish between look-alike lesions (mesothelioma vs. carcinoma, for example), or divine the cellular lineage of extremely undifferentiated neoplasms (lymphoma vs. other small blue cell tumors).<sup>14</sup> It can also be used to highlight the presence of otherwise easily overlooked microscopic foci of tumor, such as micrometastases lurking in lymph nodes, and can be used to measure quantitatively the levels of diagnostically or prognostically important markers such as estrogen- and progesterone-receptors, and now, Her2-neu expression, in breast cancers, p53, ki-67, and a host of others.<sup>15</sup>

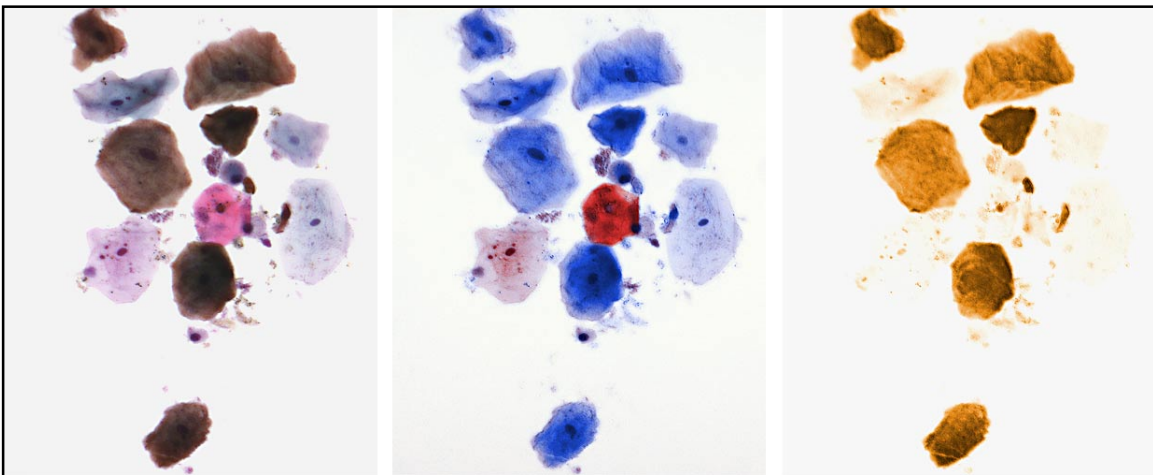


**Figure 6.** Spectral analysis of Papanicolaou- and AE3-stained sputum cells. Using linear combination analysis, the signal from the brown chromogen can be quantitatively extracted from the image. **A:** RGB-image showing how the immunostain obscures cellular morphological detail. **B:** AE3-signal digitally removed, showing cellular morphology. **C:** Chromogen signal alone, suitable for quantitation.

There are increasing indications for multicolor simultaneous staining. However, interpretation of multiply stained images is difficult, since it can be hard-to-impossible to judge, by eye or even by video camera with color-based software, whether and where more than one color overlap. Quantitation, even when only a single chromogen is present, can also be tricky when, as is frequently the case, a counterstain is used.<sup>16</sup> Computerized image analysis of such scenes has long been under development, prompted in part by research showing that interobserver variability in assessing immunostain intensity can be a considerable.<sup>17</sup> However, several technical and practical problems arise with such systems. First, the fidelity and consistency of RGB-based systems can be disappointing. Section-to-section variability, along with interactions with camera controls such as automatic gain control, can induce fluctuations in the image quality. Because the

color of a stained object is a product of the stain's transmittance and the camera's spectral response, it is possible that dyes differing in spectral properties could be sensed similarly by the camera and thus be indistinguishable. Finally, the spatial resolution of single-chip color CCD cameras is lower than that of monochrome cameras with the same pixel count because of the color mask and interpolation routines that merge information from 3 or more pixels when determining RGB and intensity values.

Spectral imaging can provide the necessary spectral resolution to detect and resolve multiple stains. In a recent publication, Ornberg et al. describe using a CRI VariSpec™ tunable filter to identify optimal wavelengths for separating signal from background in samples stained with a single chromogen plus background stain.<sup>18</sup> Using a simple processing routine, the authors were able to collect 2-3 images per minute. Zhou et al., using spectral decomposition in multispectral images, were able to resolve stain intensities in double- and triple-labeled prostate cancer specimens. However, the previous lack of convenient and affordable spectral imaging instruments has hindered the widespread adoption of this kind of approach.

We used a CRI VariSpec to acquire spectral images of sputum immunostained for cytoskeletal proteins using a brown chromogen for read-out and counterstained with the Papanicolaou stain (Figure 6). Using linear combination algorithms, we were able to separate the brown stain from the blue and red Pap-stain colors and present them individually. This allows both quantitative evaluation of immunostain intensity and qualitative assessment of the underlying morphology.

### *Conclusion: Beyond Red, Green and Blue*

Previous limitations in color imaging can now be overcome due to recent developments in spectral imaging hardware, coupled with the evolution of software tools to deal with the resulting high-dimensionality datasets. New possibilities have opened up for scientific and clinical biomedical imaging; the challenge is to explore them all.

### *References*

1. Garini, Y, Katzir, N, Cabib, D, Buckwald, RA, Soenksen, DG and Malik, Z. Spectral Bio-Imaging. 1996. In: X.F. Wang and B. Herman (Editors), *Fluorescence Imaging Spectroscopy and Microscopy. Chemical Analysis Series*. 137 John Wiley & Sons, Inc.
2. Wachman, ES, Niu, W and Farkas, DL. AOTF microscope for imaging with increased speed and spectral versatility. *Biophysical Journal* 1997; 73:1215-1222.
3. Hoyt, C. Liquid crystal tunable filters clear the way for imaging multiprobe fluorescence. *Biophotonics International* 1996; July/August:49-51.
4. Castleman, KR. *Digital image processing*. 1996, . Prentice Hall, Upper Saddle River, 667 pp.
5. Theodoridis, S and Koutroumbas, K. *Pattern recognition*. 1999, . Academic Press, San Diego, 625 pp.
6. Schrock, E, du Manoir, S, Veldman, T, Schoell, B, Wienberg, J, Ferguson-Smith, MA, Ning, Y, Ledbetter, DH, Bar-Am, I, Soenksen, D, Garini, Y and Ried, T. Multicolor spectral karyotyping of human chromosomes. *Science* 1996; 273:494-497.
7. Mark, HL and Tunnell, D. Qualitative near-infrared reflectance analysis using Mahalanobis distances. *Anal Chem* 1985; 57:1449-1456.
8. Harsanyi, JC and Chang, CI. Hyperspectral image classification and dimensionality reduction: An orthogonal subspace projection approach. *IEEE Trans Geosci Remote Sens* 1994; 32:779-785.
9. Hyv rinen, A and Oja, E. *Independent Component Analysis - a tutorial*. 1999. [http://www.cis.hut.fi/~aapo/ps/IJCNN99\\_tutorial.ps](http://www.cis.hut.fi/~aapo/ps/IJCNN99_tutorial.ps).

10. Bell, AJ and Sejnowski, TJ. Learning the higher-order structure of a natural sound. *Network* 1996; 7:261-266.
11. Hancock, PJB, Baddeley, RJ and Smith, LS. The principal components of natural images. *Network* 1992; 3:61-72.
12. Farkas, DL, Du, C, Fisher, GW, Lau, C, Niu, W, Wachman, ES and Levenson, RM. Non-invasive image acquisition and advanced processing in optical bioimaging. *Comput Med Imaging Graph* 1998; 22:89-102.
13. Frable, WJ. Needle aspiration biopsy of pulmonary tumors. *Sem Resp Med* 1982; 4:161-169.
14. Taylor, CR and Cote, RJ. Immunohistochemical markers of prognostic value in surgical pathology. *Histol Histopathol* 1997; 12:1039-1055.
15. Albonico, G, Querzoli, P, Ferretti, S, Magri, E and Nenci, I. Biophenotypes of breast carcinoma in situ defined by image analysis of biological parameters. *Pathol Res Pract* 1996; 192:117-123.
16. Karlsson, MG, Davidsson, A and Hellquist, HB. Quantitative computerized image analysis of immunostained lymphocytes. A methodological approach. *Pathol Res Pract* 1995; 190:799-807.
17. Jagoe, R, Steel, JH, Vucicevic, V, Alexander, N, Van Noorden, S, Wootton, R and Polak, JM. Observer variation in quantification of immunocytochemistry by image analysis. *Histochem J* 1991; 23:541-547.
18. Ornberg, RL, Woerner, BM and Edwards, DA. Analysis of stained objects in histological sections by spectral imaging and differential absorption. *J Histochem Cytochem* 1999; 47:1307-1314.